J Radioanal Nucl Chem (2016) 309:659–666
DOI 10.1007/s10967-015-4643-y

Usability of natural titanium-iron oxide as filler material for ionizing electromagnetic radiation shielding composites; preparation, characterization and performance

E. Eren Belgin[1] · G. A. Aycik[1] · A. Kalemtas[2] · A. Pelit[1] · D. A. Dilek[1] · M. T. Kavak[1]

Received: 31 August 2015 / Published online: 1 December 2015

Abstract In the study, usability of natural titanium-iron oxide filler for ionizing electromagnetic radiation (IEMR) shielding composites with isophthalic polyester (PES) matrix was investigated for the first time. Shielding performances of the composites were also investigated for three different IEMR energy regions as low, intermediate and high for the first time, too. Mass attenuation coefficient of prepared composite with the best shielding performance reached 80 % of elemental lead's performance at low energy regions while it had higher mass attenuation coefficient at intermediate and high energies.

Keywords Radiation shielding · Composite shield · Ilmenite · Mineral filler · Titanium oxide · Iron oxide

Introduction

Radiation exposure of human is increased by development of nuclear technology in the modern era. Consequently the need for radiation shields at different application areas is raised. Elemental lead and heavy concretes are widely used as shielding materials. But the application areas of them remains limited especially when a mobile or wearable shielding is needed because of their high weight. In addition high toxicity of elemental lead threatens human health and environment. Therefore the need for light weight and non-toxic radiation shields enhanced and improvement of superior radiation shields became an important challenge.

Light weight reduces radiation shielding performance of the material while the heavy weight materials have better performance. Thus composite materials are seem to be a good solution by combining two different materials' properties on one composite material. In a composite, a light weight material could be used as matrix material and shielding performance of the composite could be enhanced by using heavy filler materials. Polymers are one of the favorite matrix materials used for IEMR shielding because of their light weight [1–4]. Generally heavy filler materials are used with polymer matrixes like metals and metal oxides [1, 2, 4]. There are also numerous studies in which several natural minerals are used as filler materials for the composite IEMR shielding like serpentine, hematite and limonite [5–7]. A comprehensive literature review revealed that the potential IEMR shielding properties of natural mineral filled composites were investigated only with cement matrixes. Thus mineral-polymer composites and their shielding properties at different IEMR energy regions have not been exploited so far. In view of this, natural hematite filled composites were investigated for IEMR shielding applications in our previous study and challenging results were reported [7]. In the present study, a novel light weight and non toxic composite IEMR shielding material with relatively high IEMR shielding performance prepared and characterized. The natural titanium-iron oxide mineral (ilmenite) was used as filler material to increase IEMR shielding performance of the light weight polymeric matrix of the composite materials. The composites were investigated for three different IEMR energy regions by considering different interaction mechanisms of IEMR.

✉ E. Eren Belgin
ebelgin@mu.edu.tr

[1] Department of Chemistry, Mugla Sitki Kocman University, 48000 Muğla, Turkey

[2] Department of Metallurgical and Materials Engineering, Bursa Technical University, 16190 Bursa, Turkey

Experimental

In the study, commercially procured unsaturated polyester (PES) was used as composite matrix. PES is a thermoset polymer with low density (1.15 g cm^{-3}), low volumetric shrinkage, good strength/density ratio, low cost of raw material and production. PES was procured as PES resin in styrene monomer and role of it was to provide load-stress transfer and to give light weight, easy formability and processability to the composite.

The natural ilmenite in the major chemical form of $Fe^{+2}TiO_3$ (Z_{Fe}:26, Z_{Ti}:22, Z_O:8) was procured commercially and used as composite filler material for increasing IEMR shielding performance of the composite. The ilmenite has density of 4.72 g cm^{-3} and hexagonal crystal structure (Fig. 1).

A wavelength dispersive X-ray fluorescence (XRF, Rigaku ZSX Primus) instrument was used for determination of chemical analysis of the ilmenite since it is procured as natural mineral ores and generally some impurities like Mn, Mg and V are coexist beside $Fe^{+2}TiO_3$ content of the mineral in nature. Chemical analysis were performed on glass tablets prepared by fluxing powder ilmenite with $Li_2B_4O_7$ in 1:10 weight ratio. ZSX software was used for the calculation of the semi-quantitative results. The XRF analysis results of the ilmenite filler as oxides is given in Table 1.

According to the XRF analysis results approximately 59 % of the ilmenite was TiO_2 while approximately 24 % of it was Fe_2O_3 and major impurity was V_2O_5 ($\sim$12 %). There are also some other impurities beside these major constituents. Particle size and distribution analysis (Malvern Mastersizer 2000) was also performed for the ilmenite filler. It was determined that 90 % of the particles had particle size below 7.4 μm, 50 % had particle size below 2.2 μm and 10 % of them had particle size below 0.9 μm as it is seen in particle size distribution figure (Fig. 2).

Table 1 XRF analysis results of ilmenite as oxides

Oxide	wt%	Oxide	wt%
TiO_2	58.73 ± 0.0	MgO	0.44 ± 10
Fe_2O_3	24.23 ± 0.0	P_2O_5	0.13 ± 4.9
V_2O_5	11.65 ± 1.1	CaO	0.19 ± 5.9
Al_2O_3	1.81 ± 1.5	ZrO_2	0.09 ± 4.0
SiO_2	1.54 ± 1.2	Nb_2O_5	0.09 ± 0.4
MnO	1.05 ± 1.0	PbO	0.05 ± 18

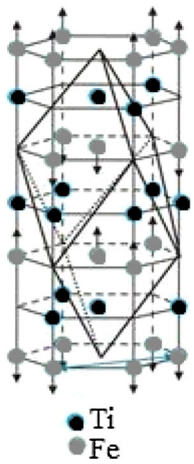

Fig. 1 Hexagonal crystal structure of ilmenite [8]

The composites were prepared for five different filler loadings between 10 and 50 % by performing a free radical polymerization process for PES resin after preliminaries of the filler. A closed mould casting technique was used for molding of the composites. The details of the preparation and molding techniques were already reported [7].

After preparation, densities of the composites were evaluated by using Archimedes' density measurement equipment [9] and the theoretical densities of the composites were calculated [10]. Then, scanning electron microscope (SEM-JEOL-JSM-7600F) examination were performed for both fractured and polished surfaces of the composites in order to understand dispersibility of ilmenite with polymer matrix, microstructure of the composites, and binding behavior between the filler particles and polymer matrix. The composites were also investigated by using Fourier transform infrared spectroscopy (FTIR-Thermo Scientific-Nicolet-1510) analysis to understand binding behavior and nature of the interaction between filler particles-matrix.

A 110 cm^3 well-type gamma spectrometer with a HPGe detector was used for IEMR shielding performance measurements of the composites. Resolution of the system was 3.78 keV at 1.33 MeV gamma-ray peak of ^{60}Co. The performance measurements were carried out for 60, 88, 122, 166, 392, 662, 898, 1173, 1333, 1836 keV gamma energies by using mixed point gamma-source containing ^{241}Am, ^{109}Cd, ^{57}Co, ^{139}Ce, ^{113}Sn, ^{137}Cs, ^{88}Y and ^{60}Co radionuclides. Wide dispersion of these single and clear gamma photopeak energies let evaluation of the results for different IEMR energy regions. After gamma spectrometric measurements linear (μ_L) and mass (μ_M) attenuation coefficients and half value layers (HVL) were calculated for the composites and also pure lead (the most widely used shielding material) for comparison. The details of the shielding performance measuring and calculation procedure were already reported [7].

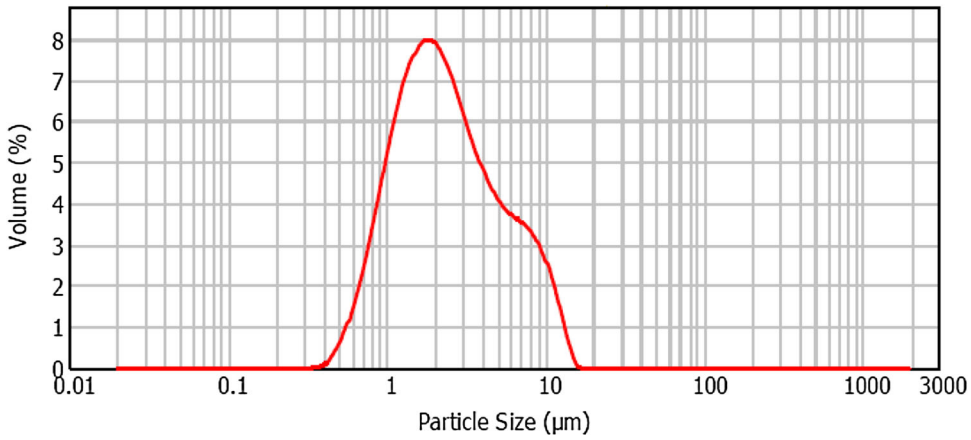

Fig. 2 Particle size distribution of ilmenite filler

Results and discussion

Density and microstructure of the composites

The used composite matrix material was a light weight polymer thus an increment in the filler loading increased Z number and also density of the composite material [1] because of dispersion of the high density filler materials within the low density matrix, as it was expected (Table 2).

The experimental and theoretical densities of the composites were found to be in good agreement. It was another inference due to Table 2 that there were still enough polymer that could cover all the filler surfaces although 50 % filler loadings. Thus it means critical filler loading value was not exceeded that could increase free volume and decrease density of the composites [10].

The micrographs determined by SEM studies for the polished (a, b) and fractured (c, d) surfaces of the IPES-50 (the composite with best IEMR shielding performance) are shown in Fig. 3.

The most important parameters that must be satisfied for producing a composite material are homogeneous dispersion of filler particles in the matrix and good adhesion between the interfaces of the matrix and filler particles. Thus the aim of the SEM studies was investigation of these parameters. In Fig. 3a it is seen that there is a homogeneous dispersion of filler particles within the matrix. Coagulated regions of filler particles were not observed. On the other hand in Fig. 3b there are some coagulated areas were observed at the upper sides of the micrograph. It was not an unexpected situation that as the particle size of the filler decreases homogeneous distribution of the particles within the matrix becomes harder. Thus the filler particles had lower particle size at the coagulated areas.

Energy dispersive X-ray analysis (EDS) was also carried out for point elemental analysis and elemental mapping at the polished surface of the composite seen in Fig. 3 and elemental analysis results are given in Table 3.

The EDS results confirmed that the matrix of the composites were seen in dark colors (b1, d1) and the light colored regions (b2, d2) were filler particles regions in Fig. 3. Approximately 71 % of b1 was carbon atom that was the major component of the polymer matrix on the other hand titanium, iron and oxygen atoms were the major components of the filler particles with the chemical formula of $Fe^{+2}TiO_3$ with approximately 87 %. The palladium contents were caused by the coating of the SEM samples. EDS mapping studies were also done for the polished surface and the homogeneous dispersion of the elements were confirmed.

In Fig. 3c, there were not many filler particle holes at the fractured surfaces of the composite except some confined areas of the fractured surface (d1), these holes could be avoided by surface treatment of the filler particles.

Table 2 Sample designations, filler loading percentages and experimental/theoretical densities of the prepared composites

Sample designation	Filler concentration of composite (%)	Experimental density (g cm^{-3})	Theoretical density (g cm^{-3})
IPES-10	10	1.31 ± 0.00	1.24
IPES-20	20	1.41 ± 0.00	1.35
IPES-30	30	1.53 ± 0.00	1.49
IPES-40	40	1.67 ± 0.00	1.65
IPES-50	50	1.86 ± 0.00	1.85

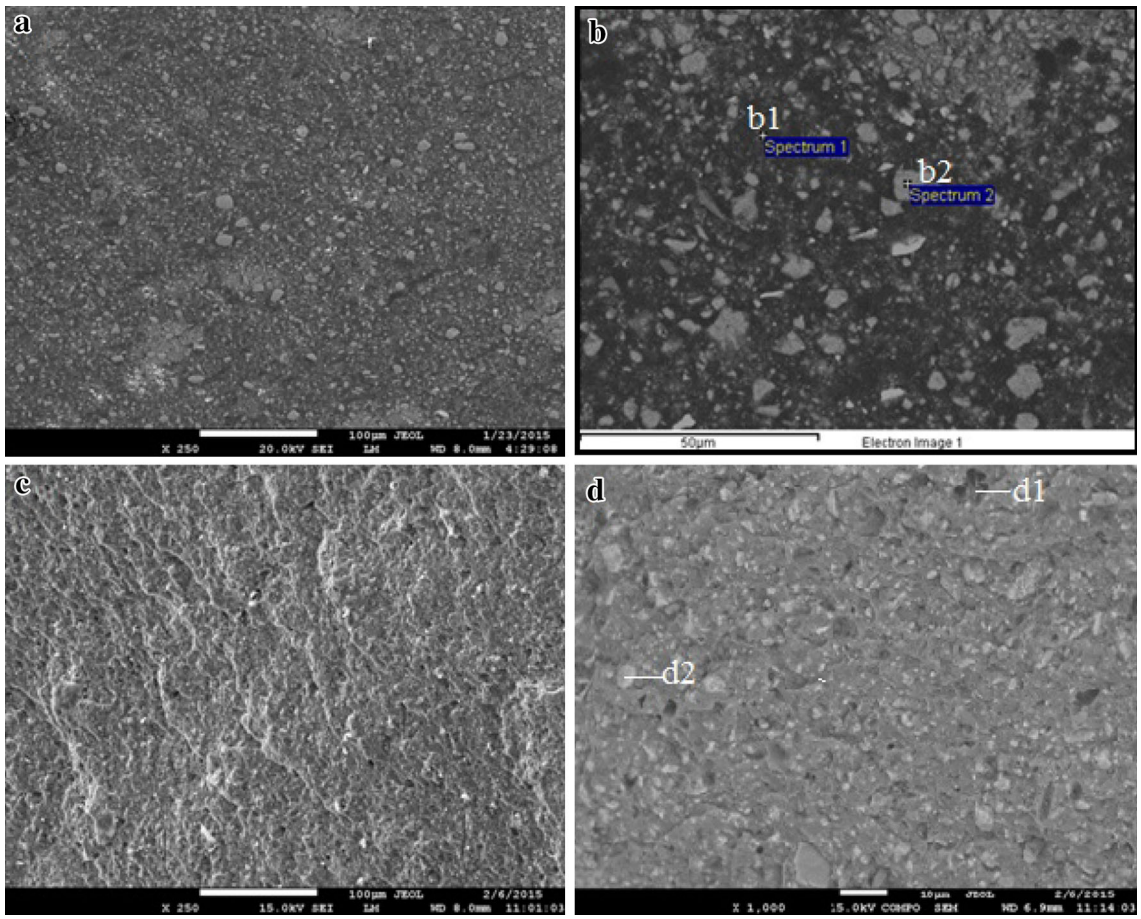

Fig. 3 SEM micrographs of IPES-50 for polished surface (**a** ×250, **b** ×1000) and fractured surface (**c** ×250, **d** ×1000)

Table 3 EDS results for polished surface (Fig. 2b) of the composite at different points

Region	Carbon (atomic%)	Oxygen (atomic%)	Iron (atomic%)	Titanium (atomic%)	Aluminum (atomic%)	Manganese (atomic%)	Palladium (atomic%)
b1	70.89	18.15	2.74	7.23	–	–	0.99
b2	10.44	58.45	6.01	22.18	0.37	1.03	1.51

Because if there is of poor adhesion between matrix and filler particles there should be some holes on the surface that could take shape in the fracture instant [11].

The FTIR spectrums of the composite matrix PES and IPES50 are given in Fig. 4. The absorption bands corresponding to the C–H bonds and C=O bonds at 2962 and 1719 cm^{-1} [12] are seen in both spectrums.

The FTIR spectrum of 50 % ilmenite filled composite IPES50 was also in good agreement with pure PES as shown in Fig. 4. Thus it was thought that there was only physical interaction between ilmenite particles and PES matrix thus the functional group intensity of the PES was not changed by the addition of the filler.

IEMR attenuation performances of the composites

The μ_L, μ_M and HVL values of the prepared composites and elemental lead were calculated and results are given in Table 4.

The linear dependence of determined μ_L values on densities of the composites is shown in Fig. 5. The dependences shown in Fig. 5 were plotted by using mean μ_L values for low (mean of 60, 88, 122, 166, 392 keV results), intermediate (mean of 662, 898 keV results) and high (mean of 1173, 1333, 1836 keV results) energy regions.

Figure 5 was indicated another phenomena that as the IEMR energy increases the density of the shielding mate-

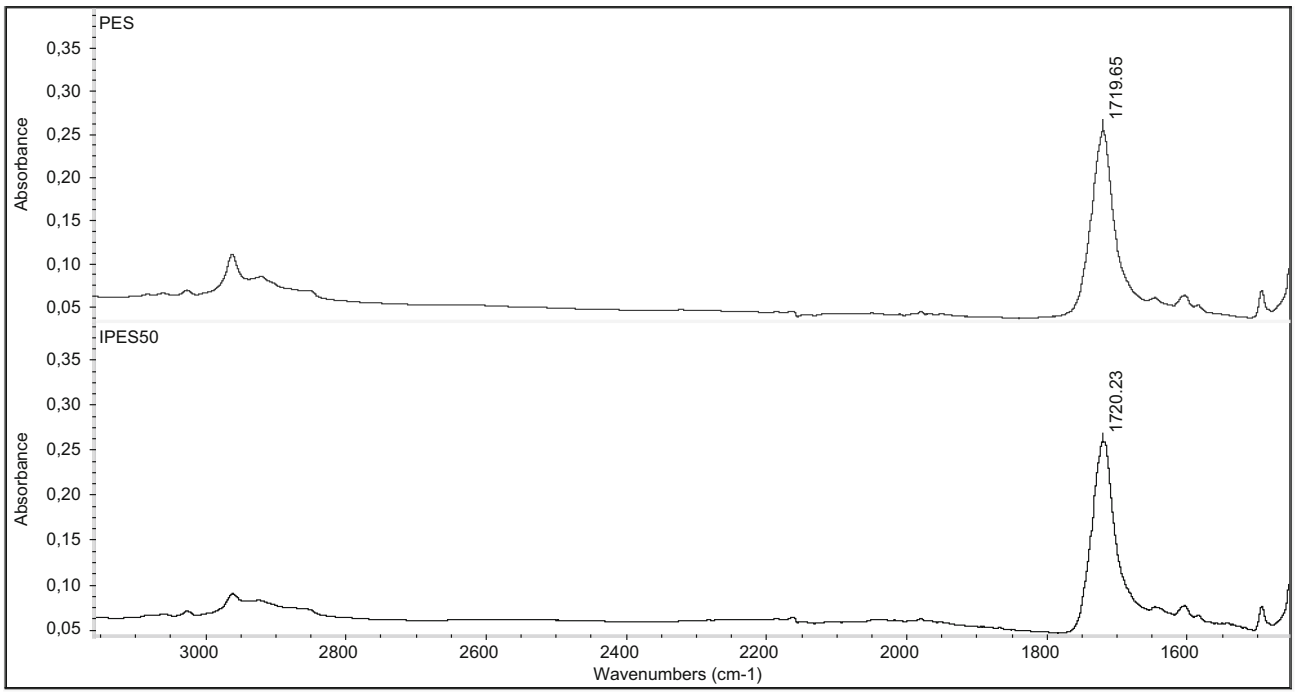

Fig. 4 FTIR spectrums of the PES and IPES50

rial became ineffective on attenuation performance because of the different interaction mechanisms of IEMR with matter at different IEMR energies. While the predominant interaction mechanism differs according to IEMR energy, the dependence of interaction on atomic number (Z) of the interacting material differs as it is summarized in Table 5.

Interaction mechanisms cannot be separated by certain energy boundaries thus Table 5 shows only predominant interactions beside other types. As a result it is a logical way to examine shielding performances of a material for different energy regions since the predominant interaction process is proportional Z^5 for low, Z for intermediate and Z^2 for high IEMR energy regions [13]. Thus in the study, as the density of the composites increased shielding performance of them are also increased sharply at low energy regions. On the other hand as the IEMR energy increased this performance increment became ineffective on the μ_L values of the composites. The insignificantly increment of μ_L values in high energy region can be attributed to several Compton scatterings beside the increasing interaction character of pair production [14]. The same behaviors of the μ_L values were also observed at the previous studies [7].

μ_M of a material is another way to express attenuation property of the material and it is independent of actual density and physical state of the material (attenuation per gram of material). Thus when weight of the shielding material is an important property for the user μ_M values are good for comparing shielding materials' efficiencies. In the study μ_M value of the composite with best shielding performance (IPES-50) was compared with the most widely used shielding material elemental lead's and also several reported shielding materials' μ_M values in Table 6 at 662 keV IEMR energy. The 662 keV IEMR energy was chosen for comparison since it was the most widely studied energy in the literature.

Although it was an expected result that the low density of the composite matrix would reduce IEMR attenuation performance of the composites while providing lightness for the composite, the prepared composite with the best performance (IPES-50) provided μ_M value higher than elemental lead at 662 keV. Also, IPES-50 was superior to normal aggregate [15], barite [15], aluminum [16], copper [16] and other studied composites like the hematite filled composites [7] reported by us, previously at 662 keV. On the other hand at low IEMR energy regions μ_M values of the elemental lead incontestable higher than the prepared composites because of the high dependence of attenuation coefficients on molecular structure, binding characteristics and crystallographic structure of the absorber material especially for low energy region [17].

As a result although the prepared composites were approximately 10 times lighter than elemental lead, lead's closest packed crystal structure refers to a tightly packed and space efficient structure [18] and μ_M value of the elemental lead becomes higher (Fig. 6). In contrast, as the IEMR energy increased dependence of attenuation on Z number decreases and the composite μ_M values becomes compatible with elemental lead. For the IEMR energies in

Table 4 Determined μ_L, μ_M and HVL values of the prepared composites and elemental lead

Sample designation		Low IEMR energy					Intermediate IEMR energy		High IEMR energy		
		60 keV	88 keV	122 keV	166 keV	392 keV	662 keV	898 keV	1173 keV	1333 keV	1836 keV
μ_L (cm^{-1})	LEAD	10.2 ± 2 %	4.05 ± 2 %	9.09 ± 2 %	8.51 ± 2 %	2.62 ± 2 %	1.13 ± 2 %	0.78 ± 2 %	0.63 ± 2 %	0.60 ± 2 %	0.51 ± 2 %
	IPES-10	0.33 ± 4 %	0.24 ± 4 %	0.27 ± 4 %	0.24 ± 4 %	0.19 ± 4 %	0.16 ± 4 %	0.02 ± 4 %	0.12 ± 4 %	0.07 ± 4 %	0.05 ± 4 %
	IPES-20	0.38 ± 4 %	0.26 ± 4 %	0.28 ± 4 %	0.33 ± 4 %	0.17 ± 4 %	0.16 ± 4 %	0.07 ± 4 %	0.12 ± 4 %	0.08 ± 4 %	0.06 ± 4 %
	IPES-30	0.53 ± 4 %	0.32 ± 4 %	0.38 ± 4 %	0.35 ± 4 %	0.17 ± 4 %	0.16 ± 4 %	0.10 ± 4 %	0.13 ± 4 %	0.10 ± 4 %	0.06 ± 4 %
	IPES-40	0.80 ± 4 %	0.35 ± 4 %	0.46 ± 4 %	0.43 ± 4 %	0.20 ± 4 %	0.23 ± 4 %	0.11 ± 4 %	0.13 ± 4 %	0.11 ± 4 %	0.09 ± 4 %
	IPES-50	0.82 ± 4 %	0.46 ± 4 %	0.47 ± 4 %	0.43 ± 4 %	0.25 ± 4 %	0.21 ± 4 %	0.18 ± 4 %	0.17 ± 4 %	0.12 ± 4 %	0.11 ± 4 %
μ_M (cm^2 g^{-1})	LEAD	0.90 ± 2 %	0.36 ± 2 %	0.80 ± 2 %	0.75 ± 2 %	0.23 ± 2 %	0.10 ± 2 %	0.07 ± 2 %	0.06 ± 2 %	0.05 ± 2 %	0.05 ± 2 %
	IPES-10	0.25 ± 4 %	0.18 ± 4 %	0.21 ± 4 %	0.18 ± 4 %	0.15 ± 4 %	0.12 ± 4 %	0.02 ± 4 %	0.09 ± 4 %	0.06 ± 4 %	0.04 ± 4 %
	IPES-20	0.27 ± 4 %	0.19 ± 4 %	0.20 ± 4 %	0.23 ± 4 %	0.12 ± 4 %	0.11 ± 4 %	0.05 ± 4 %	0.08 ± 4 %	0.06 ± 4 %	0.04 ± 4 %
	IPES-30	0.35 ± 4 %	0.21 ± 4 %	0.25 ± 4 %	0.23 ± 4 %	0.11 ± 4 %	0.11 ± 4 %	0.07 ± 4 %	0.08 ± 4 %	0.06 ± 4 %	0.04 ± 4 %
	IPES-40	0.48 ± 4 %	0.21 ± 4 %	0.27 ± 4 %	0.26 ± 4 %	0.12 ± 4 %	0.14 ± 4 %	0.07 ± 4 %	0.08 ± 4 %	0.06 ± 4 %	0.05 ± 4 %
	IPES-50	0.44 ± 4 %	0.25 ± 4 %	0.25 ± 4 %	0.23 ± 4 %	0.13 ± 4 %	0.12 ± 4 %	0.10 ± 4 %	0.09 ± 4 %	0.06 ± 4 %	0.06 ± 4 %
HVL (cm)	LEAD	0.07 ± 2 %	0.17 ± 2 %	0.08 ± 2 %	0.08 ± 2 %	0.27 ± 2 %	0.61 ± 2 %	0.89 ± 2 %	1.10 ± 2 %	1.15 ± 2 %	1.37 ± 2 %
	IPES-10	2.09 ± 4 %	2.88 ± 4 %	2.57 ± 4 %	2.92 ± 4 %	3.61 ± 4 %	4.32 ± 4 %	29.1 ± 4 %	5.89 ± 4 %	9.35 ± 4 %	14.8 ± 4 %
	IPES-20	1.84 ± 4 %	2.63 ± 4 %	2.51 ± 4 %	2.10 ± 4 %	4.10 ± 4 %	4.31 ± 4 %	9.92 ± 4 %	5.85 ± 4 %	8.19 ± 4 %	11.8 ± 4 %
	IPES-30	1.31 ± 4 %	2.18 ± 4 %	1.82 ± 4 %	1.99 ± 4 %	4.01 ± 4 %	4.28 ± 4 %	6.79 ± 4 %	5.44 ± 4 %	7.22 ± 4 %	11.2 ± 4 %
	IPES-40	0.87 ± 4 %	1.97 ± 4 %	1.52 ± 4 %	1.62 ± 4 %	3.47 ± 4 %	3.00 ± 4 %	6.23 ± 4 %	5.15 ± 4 %	6.57 ± 4 %	7.72 ± 4 %
	IPES-50	0.84 ± 4 %	1.51 ± 4 %	1.47 ± 4 %	1.61 ± 4 %	2.83 ± 4 %	3.23 ± 4 %	3.87 ± 4 %	4.01 ± 4 %	5.81 ± 4 %	6.23 ± 4 %

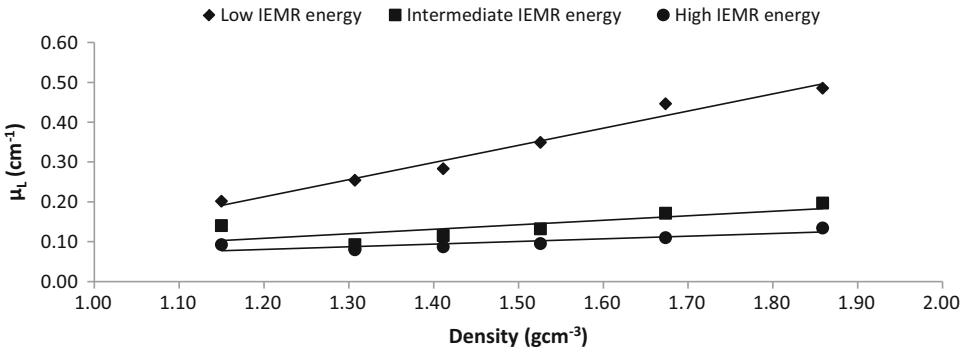

Fig. 5 Plot of linear dependence of μ_L values on density of ilmenite filled composites

Table 5 Summary of predominant interaction mechanisms and cross section equations according to IEMR energy

IEMR energy (keV)	Predominant interaction mechanism	Dependency on Z of interacting material and related cross section equation
~0 to 500	Photoelectric effect	$\sim Z^5$ (Z^n/E^3) where $n = 3$–5
~500 to 1020	Compton effect	$\sim Z$ (Z/E)
~>1020	Pair production	$\sim Z^2$ (Z $\ln(E^{-1.02})$)

Table 6 The comparison of μ_M values of various shielding materials reported in the literature

Shielding material	Reported μ_M (cm^2 g^{-1}, 662 keV)
Lead	0.100 ± 2 % (This study)
IPES-50	0.120 ± 4 % (This study)
HPES-50	0.098 ± 4 % [7]
Normal aggregate	0.081 [15]
Barite	0.076 [15]
Aluminum	0.075 [16]
Copper	0.075 [16]
50 % PbO + 50 % B_2O_3	0.088 [10]
85 % barite + 15 % colemanite	0.077 [15]

the energy range of 500–1100 keV and >1100 keV all the ilmenite filled composites had higher μ_M values than elemental lead (Fig. 6).

Conclusions

Natural titanium-iron oxide reinforced and polyester based non-toxic ionizing electromagnetic radiation shielding composites were prepared. Density evolution and SEM studies confirmed that filler particles dispersed uniformly with the matrix and critical filler loading was not exceeded. The prepared composites showed good IEMR shielding performances that increase with increasing filler loadings.

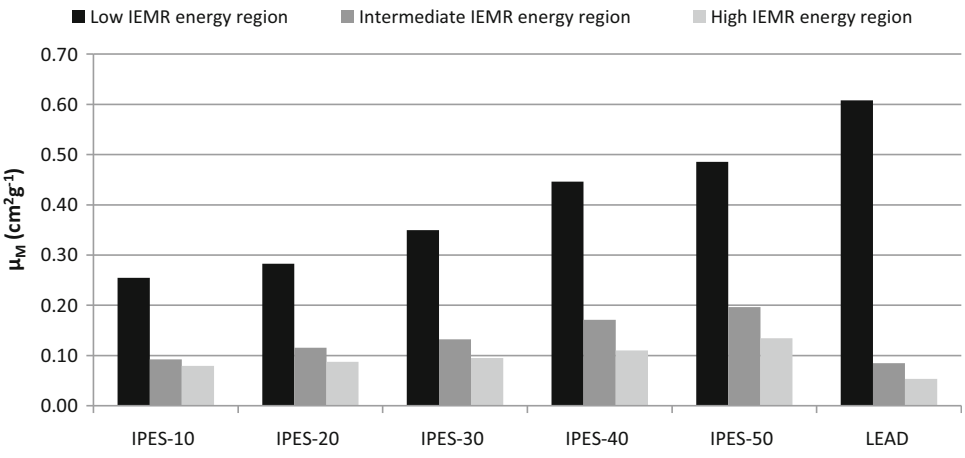

Fig. 6 Determined μ_M values of the prepared composites and elemental lead at different IEMR energy regions

The μ_M value of the composite with best shielding performance reached 80 % of the elemental lead's performance for low energy region. This performance reached approximately two times greater percentage for intermediate and high energy regions. The results also showed that density and chemical structure of the shielding material becomes ineffective on IEMR shielding as the IEMR energy raised.

Acknowledgments The authors would like to acknowledge the financial assistance of the Scientific and Technical Research Council of Turkey (TUBITAK) through Grant 213M323 December 2013 and Mugla Sitki Kocman University through the Grant 2014/003 February 2014.

References

1. Plionis AA, Garcia SR, Gonzales ER, Porterfield DR, Peterson DS (2009) Replacement of lead bricks with non-hazardous polymer-bismuth for low-energy gamma shielding. J Radioanal Nucl Chem 282:239–242
2. Gwaily SE, Madani M (2002) Lead-natural rubber composites as gamma radiation shields. II: high concentration. Polym Compos 23:495–499
3. Mheemeed AK, Hasan HI, Al-Jomaily FM (2011) Gamma-ray absorption using rubber-lead mixtures as radiation protection shields. J Radioanal Nucl Chem 291:653–659
4. Eren Belgin E, Aycik GA (2015) Preparation and radiation attenuation performances of metal oxide filled polyethylene based composites for ionizing electromagnetic radiation shielding applications. J Radioanal Nucl Chem. doi:10.1007/s10967-015-4052-2
5. Bashter II, Makarious AS, El-Sayed Abdo A (1996) Investigation of hematite-serpentine and ilmenite-limonite concretes for reactor radiation shielding. Ann Nucl Energy 23:65–71
6. Kansouh WA (2012) Radiation distribution through serpentine concrete using local materials and its application as a reactor biological shielding. Ann Nucl Energy 47:258–263
7. Eren Belgin E, Aycik GA, Kalemtas A, Pelit A, Dilek DA, Kavak MT (2015) Preparation and characterization of a novel ionizing electromagnetic radiation shielding material: hematite filled polyester based composites. Radiat Phys Chem 115:43–48
8. Ilmenite lattice. http://www.metphys.mat.ethz.ch/research/mms/his. Accessed 12 Oct 2015
9. Kirdsiri K, Kaewkhao J, Pokaipisit A, Chewpraditkul W, Limsuwan P (2009) Utilization of ilmenite/epoxy composite for neutrons and gamma rays attenuation. Ann Nucl Energy 36:1360–1365
10. Harish V, Nagaiah N, Niranjana Prabhu T, Varughese KT (2008) Preparation and characterization of lead monoxide filled unsaturated polyester based polymer composites for gamma radiation shielding applications. J Appl Polym Sci 112:1503–1508
11. El-Sarraf MA, El-Sayed Abdo A (2013) Influence of magnetite, ilmenite and boron carbide on radiation attenuation of polyester composites. Radiat Phys Chem 88:21–26
12. Settle F (1997) Handbook of instrumental techniques for analytical chemistry. Prentice Hall PTR, Upper Saddle River
13. Friedlander G, Kennedy JW, Macias ES, Miller JM (1981) Nuclear and radiochemistry. Wiley, New York
14. El-Sayed Abdo A, El-Sarraf MA, Gaber FA (2003) Utilization of ilmenite/epoxy composite for neutrons and gamma rays attenuation. Ann Nucl Energy 30:175–187
15. Demir F, Budak G, Sahin R, Karabulut A, Oltulu M, Un A (2011) Determination of radiation attenuation coefficients of heavyweight and normal-weight concretes containing barite for 0.663 MeV γ-rays. Ann Nucl Energy 38:1274–1278
16. LeClair P (2010) Gamma ray attenuation. Available at http://faculty.mint.ua.edu/~pleclair/PH255/templates/formal/formal.pdf
17. El-Enany N, El-Kameesy SU, Miligy Z, Ayad MA, Al-Kanawi AA (1994) Practical study for the development of gamma rays shielding materials. Int J Environ Stud 46:191–197
18. Miessler GL, Tarr DA (2004) Inorganic chemistry. High Education Press, Beijing